SENSOR LOCALIZATION ERROR DECOMPOSITION: THEORY AND APPLICATIONS

Joshua N. Ash and Randolph L. Moses

Department of Electrical and Computer Engineering
Ohio State University, Columbus, OH 43210

ABSTRACT

In this paper we consider performance characterizations of self-localization algorithms for sensor networks. The location parameters have a natural decomposition into relative configuration and centroid transformation components based on the influence of measurements and prior information in the problem. A linear representation of the transformation parameter space, which includes rotations and translations, is used for decomposition of general localization error covariance matrices. The proposed decomposition may be applied to any estimator, the posterior Cramér-Rao bound (CRB) in a Bayesian setting, or a traditional CRB.

Along with the CRB itself, the relative-transformation decomposition provides insight into how external inputs effect absolute localization performance. This partitioning of error is also useful to higher level applications in a sensor network that utilize results of the localization service and must account for its uncertainty. Examples are presented and an application demonstrates the utility of relative error decomposition to the problem of angle-of-arrival estimation with sensor location uncertainty.

Index Terms— Sensor network calibration, Localization, Cramér-Rao bound, Singular Fisher information

1. INTRODUCTION

Sensor self-localization, also known as self-calibration, is a fundamental component of modern sensor networks which are typically large-scale and rapidly deployed. As such, a diverse variety of self-localization algorithms based on some form of inter-node measurements have been proposed [1]. In order to better understand how noise, deployment geometry, and measurement type affect fundamental location estimation performance, a number of authors have considered the Cramér-Rao bound (CRB) on self-localization performance (see eg. [2, 3] and references therein). In this paper we extend the general CRB analysis by providing a meaningful decomposition of localization error. In particular, we decompose the total localization error into a relative portion representing error in the estimated network shape and a transformation portion representing error in the absolute position of the relative scene. This decomposition is motivated by the fact that relative information is derived from both inter-node measurements and prior information, while transformation information comes solely from prior information.

The relative-absolute error decomposition ideas presented here may be applied to CRBs in order to better understand the efficacy of measurements and priors. The decomposition may also be applied to localization covariance matrices from any estimator in order to evaluate how the estimator performs in these domains. In addition, relative-absolute error decomposition may be useful to higher level algorithms which use the results of a localization service and wish to account for sensor position uncertainty.

In the next section we give formal definitions of relative and transformation errors in a deterministic setting and provide a linear approximation which simplifies their calculation. Randomness is then introduced, and these concepts are extended to expected error. In Section 3 we demonstrate error decomposition applied to a CRB and to maximum likelihood estimates. We also illustrate an application where the complexity of angle-of-arrival estimation is greatly reduced by using error decomposition. Finally, conclusions are given in Section 4.

2. RELATIVE AND TRANSFORMATION ERROR

2.1. Definitions

Absolute location estimates are derived from two sources of information: (1) some form of inter-node measurements, such as distances or time-difference-of-arrival measurements, and (2) prior information in the form of constraints or prior probabilities on the parameters. We refer to the "shape" of the network, without regard to absolute location and orientation, as the *relative* configuration, and when considering absolute positioning, we refer to translation and rotation of the relative scene as *transformation* information. Inter-node measurements only depend on (and thus only inform upon) the relative configuration of the nodes, whereas the prior information typically informs upon both relative configuration and global transformation information. Thus, it is natural to partition absolute coordinate estimation error into relative local-

This work was supported in part by an MIT Lincoln Laboratory Graduate Fellowship.

ization error and transformation estimation error. In this paper we only consider inter-node distance measurements for localization, however the decomposition ideas are easily extended to other measurement types [4].

Consider a planar array of N sensors where $\boldsymbol{\theta} = [x_1\ y_1\ \ldots\ x_N\ y_N]^T$ denotes the absolute location parameter vector, and let $\hat{\boldsymbol{\theta}} = [\hat{x}_1\ \hat{y}_1\ \ldots\ \hat{x}_N\ \hat{y}_N]^T$ denote a localization estimate given by some estimator. As a performance metric for this estimator we consider the sum of the squared distances between the true node locations and their estimates

$$\epsilon = \sum_{i=1}^{N} d_i^2 = ||\boldsymbol{\theta} - \hat{\boldsymbol{\theta}}||^2, \tag{1}$$

where $d_i^2 = (x_i - \hat{x}_i)^2 + (y_i - \hat{y}_i)^2$. For any given estimate $\hat{\boldsymbol{\theta}}$, there is an equivalence class of node locations that have the same shape as $\hat{\boldsymbol{\theta}}$, but differ only in rotation and translation. If the estimator did not yield the optimal transformation parameters (translation and rotation), the error in (1) can be further reduced by applying a planar transformation to the previous estimate. Let $\boldsymbol{\alpha} = [\phi_0\, x_0\, y_0]$ denote the transformation parameters, and let $T_\alpha(\hat{\boldsymbol{\theta}})$ denote the operation of rotating all points in $\hat{\boldsymbol{\theta}}$ counterclockwise by an angle ϕ_0, and then applying a rigid x-translation and y-translation by x_0 and y_0, respectively. The rotation is taken about the centroid $(\bar{x}, \bar{y})$, where $\bar{x} = N^{-1}\sum_i x_i$ and $\bar{y} = N^{-1}\sum_i y_i$.

Denote by $\boldsymbol{\alpha}_0 = \arg\min_\alpha ||\boldsymbol{\theta} - T_\alpha(\hat{\boldsymbol{\theta}})||^2$ the optimal transformation parameters, and let

$$\hat{\boldsymbol{\theta}}_r = T_{\alpha_0}(\hat{\boldsymbol{\theta}}) \tag{2}$$

denote the transformed scene estimate. As the translation and rotation components of $\hat{\boldsymbol{\theta}}$ have been optimally corrected in $\hat{\boldsymbol{\theta}}_r$, the error

$$\epsilon_r \triangleq ||\boldsymbol{\theta} - \hat{\boldsymbol{\theta}}_r||^2 \tag{3}$$

represents the relative error, or the error in the "shape" of the estimate $\hat{\boldsymbol{\theta}}$. We define the transformation error ϵ_t as the portion of the total error due to miss-estimation of the transformation parameters

$$\epsilon_t \triangleq \epsilon - \epsilon_r. \tag{4}$$

These errors are illustrated graphically in Figure 1.

The transformation space ($S(\hat{\boldsymbol{\theta}})$ in Fig. 1) is a 3-dimensional nonlinear manifold in $\mathbb{R}^{2N}$ representing all possible translations and rotations of $\hat{\boldsymbol{\theta}}$. A linear subspace interpretation of the relative-absolute decomposition is obtained by linearizing $S(\hat{\boldsymbol{\theta}})$ through the transformation operator T_α. This allows us to simplify the expressions for ϵ_r, ϵ_t and their expected values. A first-order Taylor series approximation of T_α yields

$$T_\alpha(\theta) \approx \theta + x_0\boldsymbol{v}_x + y_0\boldsymbol{v}_y + \phi_0\boldsymbol{v}_\phi, \tag{5}$$

where

$$\boldsymbol{v}_x = \begin{bmatrix}1\\0\\1\\0\\\vdots\end{bmatrix}, \boldsymbol{v}_y = \begin{bmatrix}0\\1\\0\\1\\\vdots\end{bmatrix}, \boldsymbol{v}_\phi = \begin{bmatrix}-(y_1-\bar{y})\\(x_1-\bar{x})\\-(y_2-\bar{y})\\(x_2-\bar{x})\\\vdots\end{bmatrix}. \tag{6}$$

We define the approximation $\tilde{\boldsymbol{\theta}}_r$ of $\hat{\boldsymbol{\theta}}_r$ as

$$\tilde{\boldsymbol{\theta}}_r = \hat{\boldsymbol{\theta}} + W\hat{\boldsymbol{\beta}}, \tag{7}$$

where $\hat{\boldsymbol{\beta}} = [\hat{\beta}_\phi\, \hat{\beta}_x\, \hat{\beta}_y]^T$ is the minimizer

$$\hat{\boldsymbol{\beta}} = \arg\min_{\boldsymbol{\beta}} ||\boldsymbol{\theta} - (\hat{\boldsymbol{\theta}} + W\boldsymbol{\beta})||^2 \tag{8}$$

$$= W^T(\boldsymbol{\theta} - \hat{\boldsymbol{\theta}}), \tag{9}$$

with $W = [\tilde{\boldsymbol{v}}_\phi\, \tilde{\boldsymbol{v}}_x\, \tilde{\boldsymbol{v}}_y]$, and where $\tilde{\boldsymbol{v}}_\phi, \tilde{\boldsymbol{v}}_x, \tilde{\boldsymbol{v}}_y$ represent normalized versions of the already orthogonal $\boldsymbol{v}_\phi, \boldsymbol{v}_x, \boldsymbol{v}_y$.

Thus, the linear approximation $\tilde{\epsilon}_r$ of the relative error ϵ_r is given by

$$\begin{aligned}\tilde{\epsilon}_r &\triangleq ||\boldsymbol{\theta} - \tilde{\boldsymbol{\theta}}_r||^2 \\ &= ||\tilde{\boldsymbol{w}}_r||^2\end{aligned} \tag{10}$$

and the corresponding linear approximation $\tilde{\epsilon}_t$ of the transformation error is given as

$$\begin{aligned}\tilde{\epsilon}_t &\triangleq \epsilon - \tilde{\epsilon}_r \\ &= ||\boldsymbol{\xi}||^2 - ||\tilde{\boldsymbol{w}}_r||^2 \\ &= ||\tilde{\boldsymbol{w}}_t||^2.\end{aligned} \tag{11}$$

As seen in Figure 1, the vectors $\tilde{\boldsymbol{w}}_t$ and $\tilde{\boldsymbol{w}}_r$ are simply projections of the error vector $\boldsymbol{\xi} = (\boldsymbol{\theta} - \hat{\boldsymbol{\theta}})$ onto the orthogonal subspaces $\mathcal{R}(W)$ and $\mathcal{R}(W)^\perp$, respectively.

2.2. Expected error

For an unbiased estimator $\hat{\boldsymbol{\theta}}$, we may express the expected values of the three estimation errors ϵ, $\tilde{\epsilon}_r$ and $\tilde{\epsilon}_t$ in terms of the estimator covariance matrix $\Sigma_{\hat{\theta}} = E[\boldsymbol{\xi}\boldsymbol{\xi}^T]$. Let

$$\Sigma_t = E[\hat{\boldsymbol{\beta}}\hat{\boldsymbol{\beta}}^T] = W^T\Sigma_{\hat{\theta}}W \tag{12}$$

denote the covariance matrix of the transformation coefficients, and let

$$\Sigma_r = E[\tilde{\boldsymbol{w}}_r\tilde{\boldsymbol{w}}_r^T] = (\widetilde{W}\widetilde{W}^T)\Sigma_{\hat{\theta}}(\widetilde{W}\widetilde{W}^T) \tag{13}$$

denote the covariance matrix of the error in the relative subspace $\mathcal{R}(W)^\perp$, where the columns of $\widetilde{W}$ form an orthonormal basis for $\mathcal{R}(W)^\perp$. The expected errors are

$$e \triangleq E[\epsilon] = E[\boldsymbol{\xi}^T\boldsymbol{\xi}] = \text{tr}\,\Sigma_{\hat{\theta}} \tag{14}$$

$$e_r \triangleq E[\tilde{\epsilon}_r] = E[\tilde{\boldsymbol{w}}_r^T\tilde{\boldsymbol{w}}_r] = \text{tr}\,\Sigma_r \tag{15}$$

$$e_t \triangleq E[\tilde{\epsilon}_t] = E[\tilde{\boldsymbol{w}}_t^T\tilde{\boldsymbol{w}}_t] = \text{tr}\,\Sigma_t, \tag{16}$$

and, as desired, the sum of the mean component errors equals the total: $e = \text{tr}\, [\widetilde{WW}]^T\, \Sigma_{\hat{\theta}}\, [\widetilde{WW}] = e_r + e_t$. Lower bounds on the expected total, relative, and transformation errors may be obtained by substituting a localization CRB for $\Sigma_{\hat{\theta}}$ in (12)–(16).

The Fisher information matrix J for $\boldsymbol{\theta}$ based on inter-node measurements will always be singular [5] because the components of $\boldsymbol{\theta}$ in the transformation subspace, $\mathcal{R}(W)$, cannot be estimated from measurements alone. As such, the nullspace of J always contains $\mathcal{R}(W)$. In order to regularize the estimation problem for absolute localization, constraints or prior probabilities on the parameters must be imposed [4]. From these, a constrained [6] or Bayesian [7, § 2.4.3] CRB may be calculated and substituted for $\Sigma_{\hat{\theta}}$ above.

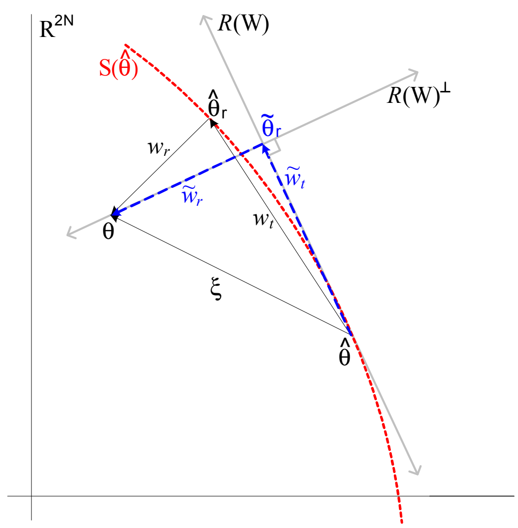

Fig. 1: Geometric illustration of relative and transformation errors in the location parameter vector $\boldsymbol{\theta}$. The manifold $S(\hat{\boldsymbol{\theta}})$ represents rigid translations and rotations of the coordinate estimates $\hat{\boldsymbol{\theta}}$, and the point on $S(\hat{\boldsymbol{\theta}})$ closest to $\boldsymbol{\theta}$ represents the optimally transformed estimate, $\hat{\boldsymbol{\theta}}_r$. The error vector $\boldsymbol{\xi} = \boldsymbol{\theta} - \hat{\boldsymbol{\theta}}$ may be decomposed into $\boldsymbol{\xi} = \boldsymbol{w}_r + \boldsymbol{w}_t$, where $\boldsymbol{w}_r = \boldsymbol{\theta} - \hat{\boldsymbol{\theta}}_r$ is the relative error vector and $\boldsymbol{w}_t = \hat{\boldsymbol{\theta}}_r - \hat{\boldsymbol{\theta}}$. $\boldsymbol{w}_t$ and $\boldsymbol{w}_r$ may be approximated, respectively, by $\tilde{\boldsymbol{w}}_t$ and $\tilde{\boldsymbol{w}}_r$, the projections of the error vector $\boldsymbol{\xi}$ onto the transformation subspace $\mathcal{R}(W)$ and the relative subspace $\mathcal{R}(W)^\perp$.

3. EXAMPLES

3.1. Error decomposition

We first demonstrate the error decomposition ideas applied to the localization of the hexagonal sensor array depicted in Figure 2. We assume that distance measurements between every pair of the six sensors are taken and that these measurements are corrupted by independent additive Gaussian noise with zero mean and standard deviation $\sigma_d = 0.5\,\text{m}$. The locations of sensors 5 and 6 are assumed to be known *a priori* in order

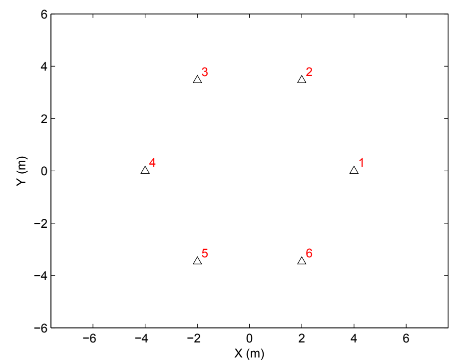

Fig. 2: Hexagonal array as a sample sensor network. Nodes 5 and 6 are anchors with known positions, while nodes 1–4 have unknown locations.

to perform localization with an absolute reference. Known-location nodes are typically referred to as anchor nodes and provide a simple form of parametric constraints.

Figure 3 illustrates a scatter plot of 1000 maximum likelihood estimates of the absolute positions of the sensors (corresponding to 1000 simulated realizations of the measurement set). The elliptical shape of the point clusters indicates obvious correlation between the x- and y-coordinate estimates for a given node, however, there is also significant correlation across nodes. To demonstrate this, each of the 1000 6-node estimates is plotted with a different greyscale intensity. For a given scene estimate, the shading of all 6 nodes was determined by the position of the estimate of node 1 (chosen arbitrarily) relative to the principle axis of cluster 1. This results in the smooth shading seen for cluster 1 in the figure. If the estimates of the other node locations were uncorrelated, their cluster estimates would appear randomly colored. However, the general trend of the shading is seen in the other clusters as well. This suggests that the variability in the *shape* of the estimated scene is actually lower than what is implied by the size of the absolute scatter plots. The decomposition ideas of this paper provide a means for quantifying this qualitative observation.

The average empirical total error ϵ, calculated as the average of ϵ over the 1000 estimates, was equal to $1.31\,\text{m}^2$. Using the anchor constraints and knowledge of the measurement type, we calculate the localization CRB, Σ_{crb}, and determined the bound on total error to be $\text{tr}\,\Sigma_{crb} = 1.30\,\text{m}$. The CRB-derived 3-$\sigma$ uncertainty ellipse for each sensor is also plotted on Figure 3. While these ellipses are good predictors of the total error distribution, they do not give a complete picture of estimation error. In particular, they fail to capture the relative error and correlation structure observed above.

For each of the 1000 scene estimates, we determine the optimally transformed relative estimate $\hat{\boldsymbol{\theta}}_r$ as in (2) and show the relative scatter plots of $\{\hat{\boldsymbol{\theta}}_r\}$ in Figure 4. The average

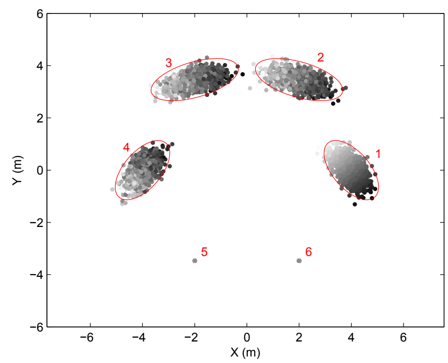

Fig. 3: Total error: Scatter plots of ML estimates of absolute positions exhibit large rotational uncertainty, as predicted by the 3-σ ellipses of the constrained CRB (–). Color coding of estimates illustrates high correlation between sensors.

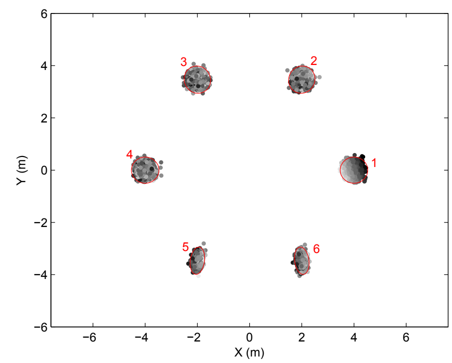

Fig. 4: Relative error: The large rotational uncertainty of Figure 3 is not seen in the optimally transformed relative estimates, $\{\hat{\boldsymbol{\theta}}_r\}$. The 3-$\sigma$ uncertainty ellipses (–) of the relative bound Σ_r accurately describe the empirical relative error.

empirical relative error ϵ_r was calculated to be $0.31\,\mathrm{m}^2$; this compares favorably to the relative portion of the constrained CRB, tr $P_W^\perp \Sigma_{crb} P_W^\perp = 0.31\,\mathrm{m}^2$, where the projection operator $P_W^\perp$ projects onto the relative subspace $\mathcal{R}(W)^\perp$. We also see in Figure 4 that the shape of the relative estimates is well-described by the relative portion of the constrained CRB, $\Sigma_r = P_W^\perp \Sigma_{crb} P_W^\perp$, and that the relative error is significantly less than the total error—as expected from the shading arguments above. In addition, there is much less correlation of localization error across nodes, as seen by the lack of shading structure in the relative estimates of Figure 4.

3.2. Application: angle-of-arrival estimation

In addition to providing insight for understand and improving localization algorithms, relative-absolute error decomposition can also be useful to higher level applications that make use of sensors with position uncertainty. In this example, we demonstrate how transformation uncertainty may be easily incorporated into a Bayesian framework for angle-of-arrival estimation. We assume that the sensor positions are described by the random vector $\boldsymbol{X} = [x_1\, y_1\, \ldots\, x_N\, y_N]^T$ which, as a result of sensor localization, is known to have distribution $p_{\boldsymbol{X}}(\boldsymbol{x})$ with mean $\boldsymbol{X}_0$ and covariance matrix Σ_X. From this sensor array, the goal is to estimate the angle-of-arrival (AOA) ω of a far-field source from a set of time-of-arrival measurements $\boldsymbol{\tau}$ of a signal emanating from that source and measured by the sensors in the network.

This problem is naturally posed in a Bayesian setting where, after the measurement $\boldsymbol{\tau}$, we have the posterior distribution $p(\omega, \boldsymbol{X}|\boldsymbol{\tau})$ from which we wish to obtain the posterior marginal

$$p(\omega|\boldsymbol{\tau}) = \int_{\mathbb{R}^{2N}} p(\omega|\boldsymbol{\tau}, \boldsymbol{x}) p_{\boldsymbol{X}}(\boldsymbol{x})\, \mathrm{d}\boldsymbol{x} \tag{17}$$

as a complete representation of our post-measurement knowledge of the AOA ω. For an N-sensor array, the integral in (17) is $2N$-dimensional. Even if the localization algorithm is nearly statistically efficient and the locations $\boldsymbol{X}$ are well-described by the Gaussian $\mathcal{N}(\boldsymbol{X}_0, \Sigma_X)$, the integral remains computationally complex and its computation impractical for a resource constrained sensor network. However, in situations where the transformation uncertainty dominates the relative uncertainty, we may approximate $p(\omega|\boldsymbol{\tau})$ by neglecting relative errors. Focusing on transformation error alone, we may also neglect unknown array translations as they do not affect far-field AOA estimates.

What remains is the rotational uncertainty of the sensor array. As such, we may approximate the array positions by their nominal value $\boldsymbol{X}_0$ along with a random rotation ϕ. Further, rotating the entire array by an angle ϕ only shifts the posterior distribution; that is, $p(\omega|\boldsymbol{\tau}, \phi) = p(\omega - \phi|\boldsymbol{\tau}, \boldsymbol{X} = \boldsymbol{X}_0)$. Therefore, the marginal in (17) may be approximated as

$$p(\omega|\boldsymbol{\tau}) \approx \int_{\mathbb{R}} p(\omega - \phi|\boldsymbol{\tau}, \boldsymbol{X} = \boldsymbol{X}_0) p(\phi)\, \mathrm{d}\phi. \tag{18}$$

Comparing the approximation (18) to (17), we see that the $2N$-dimensional integral has been reduced to a single scalar convolution.

When only $\boldsymbol{X}_0$ and Σ_X are known, we can approximate $p(\phi)$ as a Normal distribution $\phi \sim \mathcal{N}(0, \sigma_\phi^2)$, with variance σ_ϕ^2 easily calculated from the upper left element of the covariance matrix Σ_t of the transformation parameters, $(\Sigma_t)_{1,1} = E[\hat{\beta}_\phi^2]$,

$$\sigma_\phi^2 = \frac{E[\hat{\beta}_\phi^2]}{||\boldsymbol{v}_\phi||^2}. \tag{19}$$

We illustrate the technique using the sensor array of Figure 2 with Σ_X given by the CRB described in the previous section and illustrated graphically in Figure 3. In this case, (19) yields $\sigma_\phi = 3.96°$. We demonstrate using a true source

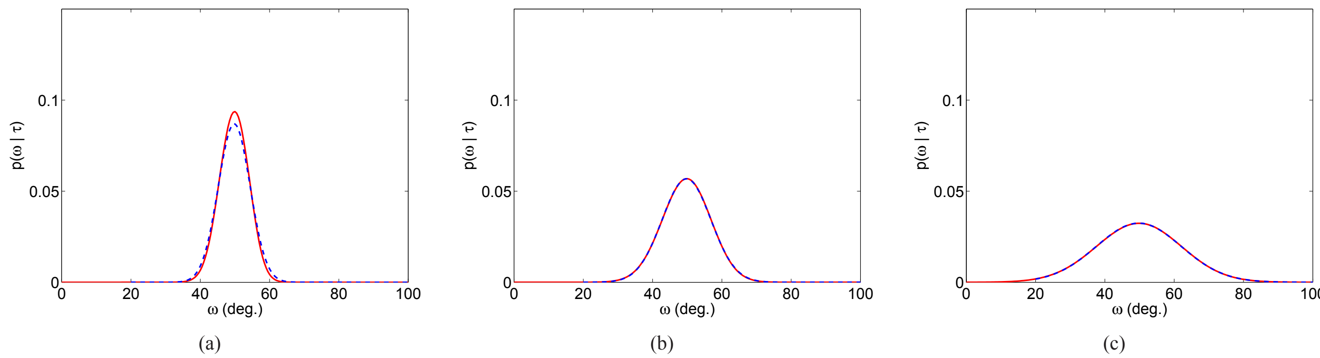

Fig. 5: Angle-of-arrival estimation. The true post-measurement distribution $p(\omega|\boldsymbol{\tau})$ of the AOA computed from the $2N$-dimensional integral (17) is plotted (—) and compared to the approximation (- -) obtained from the 1-D convolution integral (18). Three different measurement qualities are considered; $\sigma_t = 2\,\text{ms}$ (a), $\sigma_t = 5\,\text{ms}$ (b), $\sigma_t = 10\,\text{ms}$ (c). The width of $p(\omega|\boldsymbol{\tau})$ increases as the measurements grow worse, and, for the last two cases, the approximation is nearly indistinguishable from the true distribution.

AOA of $50°$ and assume that the six sensors each measure the arrival time of an acoustic signal with independent Gaussian measurement errors $\mathcal{N}(0, \sigma_t^2)$. In Figure 5 we plot the true marginal $p(\omega|\boldsymbol{\tau})$ from (17) and compare it to the convolution approximation (18) resulting from only considering rotational uncertainty. Three different measurement qualities are considered, $\sigma_t \in \{2\,\text{ms}, 5\,\text{ms}, 10\,\text{ms}\}$. For the $\sigma_t = 5\,\text{ms}$ and $\sigma_t = 10\,\text{ms}$ cases, the approximation is indistinguishable from the true marginal. For the case with the best measurements, $\sigma_t = 2\,\text{ms}$, the approximation begins to break down because, relative to the measurements, sensor uncertainty is playing a larger role in the marginal and the consequences of the approximation are more evident.

4. CONCLUSIONS

This paper presented a decomposition of localization error into relative and transformation components. This natural partitioning arose by considering how different sources of information influenced different portions of an absolute localization estimate. In particular, transformation information, which represents the translation and rotation in an absolute localization solution, is only informed upon by prior information, such as constraints. Relative information, which represents the "shape" or relative configuration of the sensors, is derived from both measurements and prior information. By considering a linearization of the rigid transformation operator, we demonstrated how a localization error covariance matrix may be decomposed into relative and transformation components. This decomposition may be applied to the error covariance matrix of a particular localization algorithm, the posterior CRB in a Bayesian setting, or a traditional CRB with constraints.

Relative-absolute error decomposition is also useful in applications relying on localization results and their associated uncertainty. We demonstrated this with an example showing how significant computational savings may be achieved in angle-of-arrival estimation by only considering transformation error. Although not explicitly considered here, error decomposition can also be used to obtain error bounds for relative-only estimation algorithms, such as classical multidimensional scaling and Isomap.

5. REFERENCES

[1] F. Gustafsson and F. Gunnarsson, "Mobile positioning using wireless networks: possibilities and fundamental limitations based on available wireless network measurements," *IEEE Signal Processing Magazine*, vol. 22, no. 4, pp. 41–53, July 2005.

[2] N. Patwari, J. Ash, S. Kyperountas, A. Hero III, R. Moses, and N. Correal, "Locating the nodes: cooperative localization in wireless sensor networks," *IEEE Signal Processing Magazine*, vol. 22, no. 4, pp. 54–69, July 2005.

[3] A. Savvides, W. Garber, R. Moses, and M. Srivastava, "An analysis of error inducing parameters in multihop sensor node localization," *IEEE Trans. Mobile Computing*, vol. 4, no. 6, pp. 567–577, 2005.

[4] J. Ash and R. Moses, "On the relative and absolute positioning errors in self-localization systems," *IEEE Trans. Signal Processing*, 2007 (in submission).

[5] R. Moses and R. Patterson, "Self-calibration of sensor networks," *Unattended Ground Sensor Technologies and Applications IV, Proc. SPIE vol. 4743*, pp. 108–119, 2002.

[6] P. Stoica and B. Ng, "On the Cramér-Rao bound under parametric constraints," *IEEE Signal Processing Lett.*, vol. 5, no. 7, pp. 177–179, 1998.

[7] H. Van Trees, *Detection, Estimation, and Modulation Theory, Part I*, Wiley, New York, 1968.